



Multiferroic properties of Y-doped BiFeO₃

Lirong Luo^a, Wei Wei^a, Xueyong Yuan^b, Kai Shen^{a,*}, Mingxiang Xu^b, Qingyu Xu^{b,c,*}

^a School of Materials Science and Technology, Nanjing University of Aeronautics and Astronautics, Nanjing 210016, China

^b Department of Physics, Southeast University, Nanjing 211189, China

^c Key Laboratory of MEMS of the Ministry of Education, Southeast University, Nanjing 210096, China

ARTICLE INFO

Article history:

Received 23 May 2012

Received in revised form 19 June 2012

Accepted 20 June 2012

Available online 28 June 2012

Keywords:

Ceramics

Ferroelectrics

Magnetic materials

Sol-gel preparation

ABSTRACT

Bi_{1.04-x}Y_xFeO₃ ceramics with x up to 0.30 were prepared by a tartaric acid modified sol-gel method. The crystal structure transformed from rhombohedral (R3c) to orthorhombic (Pn2₁a) with increasing Y doping concentration, which was confirmed by the X ray diffraction (XRD) and Raman measurements. With increasing Y doping concentration x , the leakage current was effectively suppressed, and the room temperature ferromagnetism was strongly enhanced with increasing x to 0.30. Clear room temperature ferromagnetism with saturate magnetization of about 0.31 emu/g and ferroelectric properties with 25 μ C/cm² under electric field of 120 kV/cm have been observed in orthorhombic Bi_{0.74}Y_{0.30}FeO₃, suggesting the potential multiferroic applications.

© 2012 Elsevier B.V. All rights reserved.

1. Introduction

Multiferroics refers to the materials which simultaneously exhibit at least two of the ferroic properties, such as ferroelectric, ferromagnetic and ferroelastic order parameters, in a single phase [1]. Recently, most of the researches on multiferroics focused on the magnetoelectric (ME) coupling driven by the prospect of controlling polarization by the magnetic field and magnetization by electrical field [2]. However, the multiferroic materials are very rare [3]. Till now, BiFeO₃ (BFO) is the only multiferroic material with ferroelectric and antiferromagnetic orderings above room-temperature ($T_C = 1103$ K, $T_N = 643$ K), which makes it the most promising candidate for practical applications [4]. BiFeO₃ has canted G-type antiferromagnetic spin structure with a weak ferromagnetic moment ($\sim 0.02 \mu_B/\text{Fe}$) [5], and there is a superimposed cycloidal modulation with a period of about 62 nm, thus the macroscopic magnetization has been averaged to zero [6]. The magnetization is very weak which inhibits the observation of linear magnetoelectric effect [7].

Much work has been done to improve the ferroelectric and ferromagnetic properties, such as adding small amount of additives [8], preparing epitaxial films [9]. Ion substitution with large difference in ionic radius is thought to be an effective method to

improve the ferromagnetism at room temperature [10]. The effect of transition metal ion, such as Mn [8], Y [11,12], added in BiFeO₃ with small amount have been studied. The radius of Y³⁺ (1.04 Å) is smaller than Bi³⁺ (1.17 Å) [13], which can be expected to induce lattice distortion to enhance magnetic property. But contradicted results have been reported on Y-doped BiFeO₃. Bellakki et al. reported that the magnetization increased with increasing Y concentration to 0.05 and decreased sharply with further increasing Y concentration up to 0.10 [11]. Wu et al. got better magnetic properties with Y doping concentration of 0.10 than 0.05 [12].

In this letter, we study the structural and multiferroic properties of Bi_{1.04-x}Y_xFeO₃ with x up to 0.30. A sudden improvement of ferromagnetism and better ferroelectric properties were observed with x of 0.30, which has been attributed to structural transition from rhombohedral (R3c) to orthorhombic (Pn2₁a) by Y substitution [14].

2. Experimental

Bi_{1.04-x}Y_xFeO₃ ($0 \leq x \leq 0.30$) ceramics were synthesized by a tartaric acid modified sol-gel method. The Bi(NO₃)₃·5H₂O, Fe(NO₃)₃·9H₂O, Y(NO₃)₃·5H₂O and Tartaric acid, which are analytical grade, were dissolved in distilled water in proper proportions, with excess 4% Bi for compensating the loss during sintering. The solution was dried in air at 150 °C, and then sintered at 600 °C for 2 h. The obtained powders were grinded and pressed into small discs with diameter of 13 mm, sintered at 700 °C for 30 min. The crystal structure was characterized using X ray diffraction (XRD) with Cu K α radiation. Raman measurement was performed on a Horiba Jobin Yvon LabRAM HR 800 micro-Raman spectrometer with 785 nm excitation source under air ambient condition at room temperature. The field dependent magnetization ($M-H$) was measured by a vibrating sample magnetometer. The ferroelectric polarization of the samples was measured at room temperature using Radiant Technologies' Precision II ferroelectric tester using silver paste as electrodes.

* Corresponding authors. Address: Department of Physics, Southeast University, Nanjing 211189, China (Q. Xu). Tel.: +86 25 52090600x8308; fax: +86 25 52090600x8203.

E-mail addresses: shenkai84@nuaa.edu.cn (K. Shen), xuqingyu@seu.edu.cn (Q. Xu).

3. Results and discussion

Fig. 1 shows the XRD patterns of $\text{Bi}_{1.04-x}\text{Y}_x\text{FeO}_3$ ($0 \leq x \leq 0.30$). It can be clearly seen that the BiFeO_3 exhibit R3c structure without any impurity phases. All the peaks shift to higher angles gradually with increasing doping concentration of Y, due to the smaller radius of Y^{3+} (1.04 Å) than Bi^{3+} (1.17 Å) [13]. With 0.10 Y doping, a small peak marked by the arrow can be observed which becomes stronger with increasing Y doping concentration, indicating the structural transformation. Furthermore, with increasing Y doping concentration above 0.20, the (104) and (110) peaks changes to four peaks. Similar XRD pattern has been observed by Zhang et al. in the Eu doped BiFeO_3 , which has been attributed to the orthorhombic structure with space group $\text{Pn}2_1\text{a}$ [14]. However, recently, Wu et al. attributed the orthorhombic structure of BiFeO_3 with higher Y doping concentration to space group Pnma [12]. $\text{Pn}2_1\text{a}$ space group is non-centrosymmetric [14], while Pnma space group is centro-symmetric [12]. With the observation of ferroelectricity in $\text{Bi}_{0.74}\text{Y}_{0.30}\text{FeO}_3$ which will be discussed later, we conclude that the space group for orthorhombic $\text{Bi}_{1.04-x}\text{Y}_x\text{FeO}_3$ is $\text{Pn}2_1\text{a}$.

Details of the structural evolution with ion substitution on BiFeO_3 can be expressed more explicitly through Raman spectra. Fig. 2 shows the Raman spectra of $\text{Bi}_{1.04-x}\text{Y}_x\text{FeO}_3$. According to the group theory, 13 Raman active modes can be expected for the R3c rhombohedral BiFeO_3 [15]. However, not all modes can be clearly observed at room temperature [16]. Three peaks at 140, 172, and 218 cm^{-1} can be assigned to $\text{A}_1(\text{LO})$ phonons, and peaks located at 261 and 274 cm^{-1} are associated with $\text{E}(\text{TO})$ phonons [8]. With 0.10 Y substitution, the $\text{Bi}_{0.94}\text{Y}_{0.1}\text{FeO}_3$ shows almost the same Raman spectra as BiFeO_3 , indicating that the main phase is in R3c structure. However, the peak intensities decrease, and the A_1 modes shift to higher frequency ($\text{A}_1(\text{LO})$, $\text{A}_1(2\text{LO})$, $\text{A}_1(3\text{LO})$ at 146, 174, and 223 cm^{-1} respectively). The low frequency modes of $\text{A}_1(\text{LO})$, and $\text{A}_1(2\text{LO})$ are closely related to the Bi-O bond vibrations [8]. The Raman modes shift to higher frequency with increasing pressure which compresses the lattice unit cell [17]. With further increasing Y doping concentration to 0.20, the three $\text{A}_1(\text{LO})$ and two $\text{E}(\text{TO})$ modes disappear, while the intensity of three new modes (310 , 522 and 618 cm^{-1}) becomes stronger. The Raman spectra are quite different from that of the BiFeO_3 in space group of Pnma [12]. Similar spectra have been reported by Dai et al. on Eu-doped BiFeO_3 [18]. The structural refinement has confirmed the space group of orthorhombic Eu-doped BiFeO_3 is $\text{Pn}2_1\text{a}$ [14],

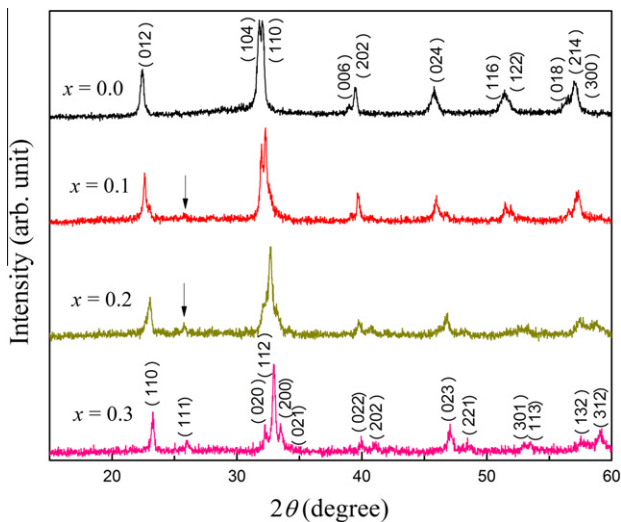


Fig. 1. XRD patterns of $\text{Bi}_{1.04-x}\text{Y}_x\text{FeO}_3$ ($x = 0, 0.10, 0.20, 0.30$).

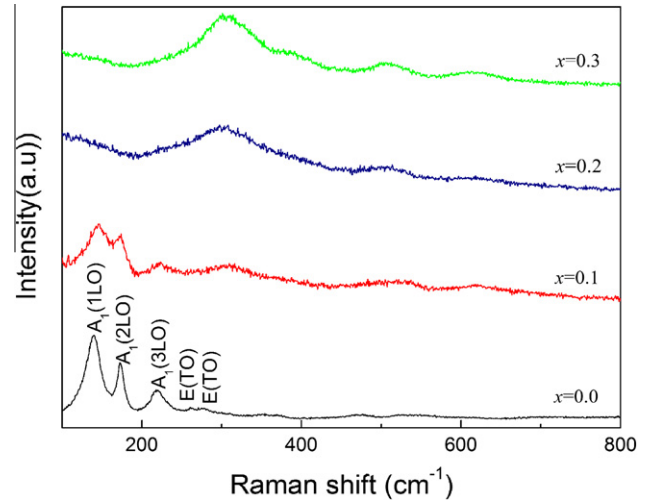


Fig. 2. Raman spectra of $\text{Bi}_{1.04-x}\text{Y}_x\text{FeO}_3$ ($x = 0, 0.10, 0.20, 0.30$).

suggesting the space group of orthorhombic $\text{Bi}_{1.04-x}\text{Y}_x\text{FeO}_3$ should be $\text{Pn}2_1\text{a}$.

Fig. 3 illustrates the room temperature $M-H$ curves of $\text{Bi}_{1.04-x}\text{Y}_x\text{FeO}_3$. Linear curve was observed for BiFeO_3 , confirming the antiferromagnetic properties. With 0.10 and 0.20 Y doping, no significant changes have been observed. With increasing x up to 0.30, a clear hysteresis loop can be observed, indicating the ferromagnetic properties. The remnant magnetization ($M_r = 0.09 \text{ emu/g}$) and saturate magnetization ($M_s = 0.31 \text{ emu/g}$) of $\text{Bi}_{0.74}\text{Y}_{0.30}\text{FeO}_3$ increase significantly compared to those values of BiFeO_3 . It should be noted that Y^{3+} is nonmagnetic ions. Thus Y doping will not contribute to the enhanced ferromagnetism directly. The observed ferromagnetism can only come from the $\text{Fe}^{3+}-\text{O}^{2-}-\text{Fe}^{3+}$ superexchange interaction. Recently, Yuan et al. studied the Y-doped LuFeO_3 , and attributed enhanced ferromagnetism to the structural modification on the FeO_6 octahedra by Y doping [19]. YFeO_3 is a canted antiferromagnet with weak saturate magnetization of about 0.18 emu/g , which is smaller than that of $\text{Bi}_{0.74}\text{Y}_{0.30}\text{FeO}_3$ (0.31 emu/g). Furthermore, the coercivity of YFeO_3 (970 Oe) is much larger than that of $\text{Bi}_{0.74}\text{Y}_{0.30}\text{FeO}_3$ (150 Oe) [20]. Thus the possible contribution from the impurity phase of YFeO_3 can be excluded, and the sudden improvement of the ferromagnetism in

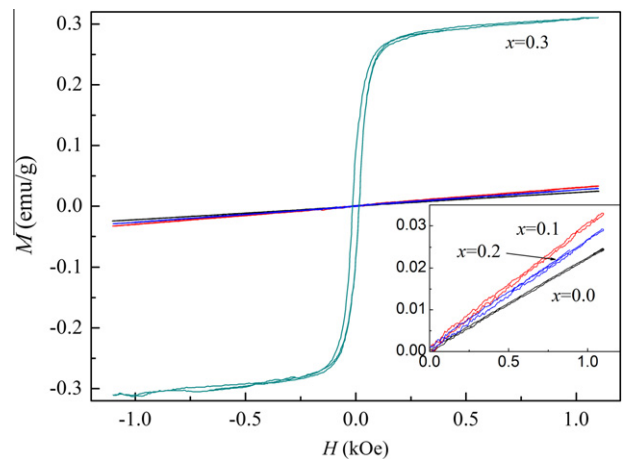


Fig. 3. Room temperature $M-H$ curves of $\text{Bi}_{1.04-x}\text{Y}_x\text{FeO}_3$ ($x = 0, 0.10, 0.20, 0.30$). The inset shows the enlarged view of the $M-H$ curves for $\text{Bi}_{1.04-x}\text{Y}_x\text{FeO}_3$ ($x = 0, 0.10, 0.20$).

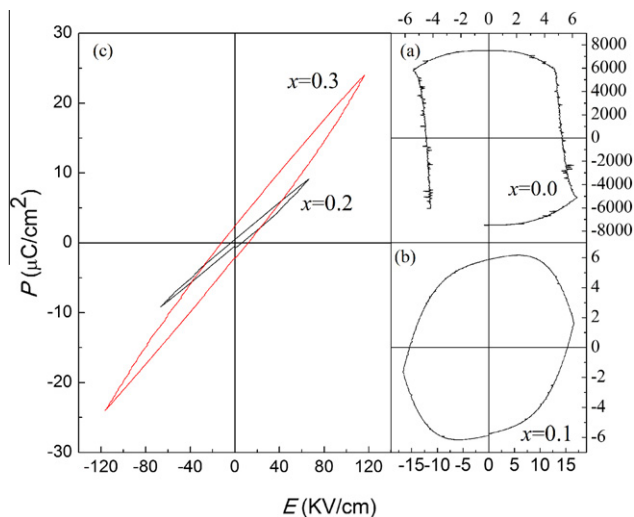


Fig. 4. Ferroelectric hysteresis loops for $\text{Bi}_{1.04-x}\text{Y}_x\text{FeO}_3$ ($x = 0, 0.10, 0.20, 0.30$) at room temperature.

$\text{Bi}_{0.74}\text{Y}_{0.30}\text{FeO}_3$ might be attributed to the suppression of the cycloidal modulation and the canted antiferromagnetic spin structure.

The ferroelectric hysteresis loops (P – E) of $\text{Bi}_{1.04-x}\text{Y}_x\text{FeO}_3$ are shown in Fig. 4. Due to the large leakage current in BiFeO_3 , P – E curve shows rounded shape with unusual large value [21]. With increasing x to 0.10, the P – E loop is still rounded in shape, but much improved in comparison with that of the undoped BiFeO_3 . With further increasing x , the leakage current was effectively suppressed, and the P – E loops became more and more typical, as shown in Fig. 4c. Similar phenomena have been observed in rare-earth (such as La, Nd, etc.) doped BiFeO_3 [22]. We were unable to obtain the exact value of the saturate polarization, due to the electrical penetration before full switching could occur, which also determine the maximum electrical field can be applied during the ferroelectric measurements. The improvement of the ferroelectric properties is due to the suppression of the leakage current, which would ascribed to the suppression of the oxygen vacancies by Y substitution for the volatile Bi [22].

4. Conclusion

In summary, $\text{Bi}_{1.04-x}\text{Y}_x\text{FeO}_3$ ($0 \leq x \leq 0.30$) ceramics were prepared by a tartaric acid modified sol–gel method. The effect of Y doping for BFO on the crystal structure, magnetic and ferroelectric properties have been investigated. XRD and Raman measurements

reveal the structural transition from rhombohedral R3c of BiFeO_3 to orthorhombic Pn2₁a with increasing x above 0.20. The doping of Y has little effect on the magnetic properties with increasing x to 0.20, while sudden improvement of ferromagnetism has been observed in $\text{Bi}_{0.74}\text{Y}_{0.30}\text{FeO}_3$. Increasing x can effectively suppress the leakage current, and clear ferroelectric hysteresis loop has been observed in $\text{Bi}_{1.04-x}\text{Y}_x\text{FeO}_3$ with $x > 0.20$. The coexistence of ferromagnetism and ferroelectricity in $\text{Bi}_{0.74}\text{Y}_{0.30}\text{FeO}_3$ suggests the potential multiferroic applications.

Acknowledgments

This work is supported by the National Natural Science Foundation of China (51172044), the National Science Foundation of Jiangsu Province of China (BK2011617), the Fundamental Research Funds for the Central Universities (NS2012110), National Key Projects for Basic Researches of China (2010CB923404), by NCET-09-0296, the Scientific Research Foundation for the Returned Overseas Chinese Scholars, State Education Ministry, and Southeast University (the Excellent Young Teachers Program and Seujq201106).

References

- [1] W. Eerenstein, N.D. Mathur, J.F. Scott, *Nature* 442 (2006) 759.
- [2] Daniel. Khomskii, *Physics* 2 (2009) 20.
- [3] S.W. Cheong, M. Mostovoy, *Nat. Mater.* 6 (2007) 13.
- [4] G. Catalan, J.F. Scott, *Adv. Mater.* 21 (2009) 2463.
- [5] V.G. Prokhorov, G.G. Kaminsky, J.M. Kim, T.W. Eom, J.S. Park, Y.P. Lee, V.L. Svetchnikov, G.G. Levchenko, Y.M. Nikolaenko, V.A. Khokhlov, *Low Temp. Phys.* 37 (2011) 129.
- [6] I. Sosnowska, T. Peterlin-Neumaier, E. Steichele, *J. Phys. C: Solid State Phys.* 15 (1982) 4835.
- [7] H. Béa, M. Bibes, S. Petit, J. Kreisel, A. Barthélémy, *Philos. Mag. Lett.* 87 (2007) 165.
- [8] J.Z. Huang, Y. Shen, M. Li, C.W. Nan, *J. Appl. Phys.* 110 (2011) 094106.
- [9] K. Ujimoto, T. Yoshimura, A. Ashida, N. Fujimura, *Appl. Phys. Lett.* 100 (2012) 102901.
- [10] Q.Y. Xu, H.F. Zai, D. Wu, T. Qiu, M.X. Xu, *Appl. Phys. Lett.* 95 (2009) 112510.
- [11] M.B. Bellakki, V. Manivannan, *J. Sol–Gel Technol.* 53 (2010) 184.
- [12] Y.J. Wu, X.K. Chen, J. Zhang, X.J. Chen, *J. Magn. Magn. Mater.* 324 (2012) 1348.
- [13] R.D. Shannon, *Acta Cryst. A* 32 (1976) 751.
- [14] Xingquan Zhang, Yu Sui, Xianjie Wang, Yang Wang, *J. Alloys Compd.* 507 (2010) 157.
- [15] P. Hermet, M. Goffinet, J. Kreisel, Ph Ghosez, *Phys. Rev. B* 75 (2007) 220102.
- [16] D. Rout, K.S. Moon, S.J.L. Kang, *J. Raman Spectrosc.* 40 (2009) 618.
- [17] Y. Yang, L.G. Bai, K. Zhu, Y.L. Liu, S. Jiang, J. Liu, J. Chen, X.R. Xing, *J. Phys. Condens. Mater.* 21 (2009) 385901.
- [18] H.Y. Dai, T. Li, R.Z. Xue, Z.P. Chen, Y.C. Xu, *J. Supercond. Nov. Magn.* 25 (2012) 109.
- [19] X. Yuan, Y. Tang, Y. Sun, M. Xu, *J. Appl. Phys.* 111 (2012) 053911.
- [20] H. Shen, J.Y. Xu, A.H. Wu, J.T. Zhao, M.L. Shi, *Mater. Sci. Eng. B* 157 (2009) 77.
- [21] D.V. Karpinsky, I.O. Troyanchuk, J.V. Vidal, N.A. Sobolev, A.L. Kholkin, *Solid State Commun.* 151 (2011) 536.
- [22] H. Uchida, R. Ueno, H. Funakubo, S. Koda, *J. Appl. Phys.* 100 (2006) 014106.